this phase, they cross at their common center of gravity, but differ by a 0.5° rotation. They are nearly perpendicular, respectively, to the $\bar{4}$ and C_2 axes considered in phase I. Finally, we must note that, at a lower precision (1.3% on distances and 2% on angles), the iron and the sulfur tetrahedra both agree with the T_d symmetry in phase II. Within the same precision, only the iron tetrahedra agree with this T_d symmetry in phase I.

Thus, it seems that overall, as the temperature is decreased through the phase transition, the structure behaves as if the iron tetrahedra were trying to approach T_d symmetry, at the expense of the organization of the "softer" sulfur atoms. Apparently, the supplementary distortion of the Fe_4S_4 core introduced by this temperature change must be a consequence of the strains due to the reorganization of the phenyls of the thiolate ligands and of the chain ends of the tetrabutylammonium ions, which drive the phase transition. However, these geometrical changes at the level of cubane cores are of small amplitude and they have no apparent influence on the electronic structure of the cubane, which, as seen by Mössbauer spectroscopy, remains the same in the two phases.

VI. Conclusion

The origin of the phase transition appears to be due to an increase of the dynamic disorder at the level of the terminal carbon atoms of the tetrabutylammonium counterions. These motional changes possibly drive, via intermolecular interactions, the observed partial reorganization of the relative orientations of the phenyl planes of the thiolate groups.

Concerning the structure of the cubane itself, we think that it is its immediate environment that imposes its low symmetry and modulates its geometry. Finally, we think that the geometry modification between the two phases must result from the interplay of the external influences exercised by the vicinal ligands and counterions and of its rather rigid internal structure, which presents however some plasticity. The geometric changes observed at the level of the cubane cores have no apparent influence on the electronic state of the system.

Acknowledgment. We thank all persons of the DRF who helped us with technical facilities and stimulating discussions. We want to thank especially P. Auric, who performed Mössbauer experiments, and B. Castaing for useful discussions on thermodynamic theory.

Registry No. $[Bu_4N]_2[Fe_4S_4(SC_6H_5)_4]$, 52586-83-1.

Supplementary Material Available: Tables of crystallographic data, positional and thermal parameters for all atoms, and angles and distances for bonds between them (32 pages); a listing of observed and calculated structure factors (18 pages). Ordering information is given on any current masthead page.

Contribution from the Istituto di Teoria e Struttura Elettronica dei Composti di Coordinazione del CNR, Area della Ricerca di Roma, P.O. Box 10, 00016 Monterotondo Stazione, Roma, Italy

Metal Complexes of the New Ligand 1,2,6,7-Tetracyano-3,5-diimino-3,5-dihydropyrrolizinide, $M^{II}(C_{11}N_7H_2)_2$, as Basic Units for Molecular Materials. Electrochemical and Metal–Phthalocyanine-Like Electronic Properties of the Nickel(II) Complex and X-ray Crystal Structures of Its Adducts with Dioxane and Tetrathiafulvalene

Mario Bonamico, Vincenzo Fares,* Alberto Flamini,* and Nicola Poli

Received October 17, 1990

The synthesis, characterization, and electrochemical behavior of the bis(1,2,6,7-tetracyano-3,5-diimino-3,5-dihydropyrrolizinido)nickel(II) complex, Ni(β-dtpy)$_2$, have been investigated. In solution it is square planar and shows a metal–phthalocyanine-like electronic structure. In the solid state it incorporates oxygenated solvent of crystallization and the nickel is hexacoordinated, as from the results of the reported X-ray crystal structure of $Ni(C_{11}N_7H_2)_2 \cdot 2H_2O \cdot 3diox$ (**3**) (diox = 1,4-dioxane). The crystal structure of the TTF and THF adduct, $Ni(C_{11}N_7H_2)_2 \cdot TTF \cdot 2THF$ (**4**), is also reported: it is a charge-transfer complex, consisting of infinite stacks of alternate donor and acceptor molecules. Both complexes crystallize in the monoclinic system. Crystal data are as follows: for **3**, $C_{34}H_{32}N_{14}NiO_8$, space group $P2_1/n$, a = 11.184 (3) Å, b = 15.682 (4) Å, c = 11.720 (4) Å, β = 110.77 (2)°, Z = 2; for **4**, $C_{36}H_{24}N_{14}NiO_2S_4$, space group $P2_1/c$, a = 11.920 (3) Å, b = 21.612 (8) Å, c = 7.979 (2) Å, β = 109.68 (2)°, Z = 2. The cyclic voltammetry of Ni(β-dtpy)$_2$ shows multistep, overlapping reduction waves from 0 to −1.5 V vs SCE. A very small concentration of the radical monoanion $Ni(\beta\text{-dtpy})_2^{\bullet-}$ can be generated in solution, as detected by EPR spectroscopy during in situ electrolysis in DMF with $LiClO_4$ as supporting electrolyte (unresolved structure signal, g = 2.0057). Nevertheless the radical monoanion can be quantitatively isolated in the solid state as $Ni(\beta\text{-dtpy})_2^{\bullet-}Et_4N^+ \cdot 3CH_3OH$ (**6**) when the electrolysis of Ni(β-dtpy)$_2$ is carried out in methanol with TEAP as supporting electrolyte. **6** is a semiconductor ($\sigma = 1.062 \times 10^{-4}$ S cm^{-1}; E_a = 0.024 eV) with the unpaired electrons partially antiferromagnetically coupled at room temperature (μ_{eff} = 1.36 μ_B). As far as the delocalization of the odd electron in $Ni(\beta\text{-dtpy})_2^{\bullet-}$ anion is concerned, both the ESR and ESCA data of **6** show that it is confined mainly to the ligand system.

1. Introduction

After our discovery[1] that the polycyanopyrrolenine anion (**1**), resulting from a reductive autocondensation of tetracyanoethylene[2] (TCNE), reacts with divalent metal ions yielding bis(β-diiminotetracyanopyrrolizinido)metal(II) complexes M(β-dtpy)$_2$ (**2**)[3] (Scheme I), we began to study complexes **2** with the aim of evaluating them as basic units for producing molecular materials such as one-dimensional conducting charge-transfer compounds, on the analogy of tetracyanoquinodimethane (TCNQ), for the

(1) Bonamico, M.; Fares, V.; Flamini, A.; Poli, N. *Angew. Chem., Int. Ed. Engl.* **1989**, *28*, 1049.
(2) Dessy, G.; Fares, V.; Flamini, A.; Giuliani, A. M. *Angew. Chem., Int. Ed. Engl.* **1985**, *24*, 426.
(3) Numbering of the compounds throughout this paper is as follows: $C_{11}N_7H_2^-$ (**1**); $M(C_{11}N_7H_2)_2 \equiv M(\beta\text{-dtpy})_2$ (**2**); $Ni(\beta\text{-dtpy})_2 \cdot 2H_2O \cdot 3diox$ (**3**); $Ni(\beta\text{-dtpy})_2 \cdot TTF \cdot 2THF$ (**4**); $Ni(\beta\text{-dtpy})_2 \cdot 2C_3H_6O$ (**5**); $Ni(\beta\text{-dtpy})_2^{\bullet-}NEt_4^+ \cdot 3CH_3OH$ (**6**); $Ni(\beta\text{-dtpy})_2 \cdot 2THF \cdot 2THF$ (**7**); $Cu(\beta\text{-dtpy})_2 \cdot 2THF$ (**8**); $Et_3NH^+TCNQ^{\bullet-}$ (**9**).

0020-1669/91/1330-3081$02.50/0

Scheme I

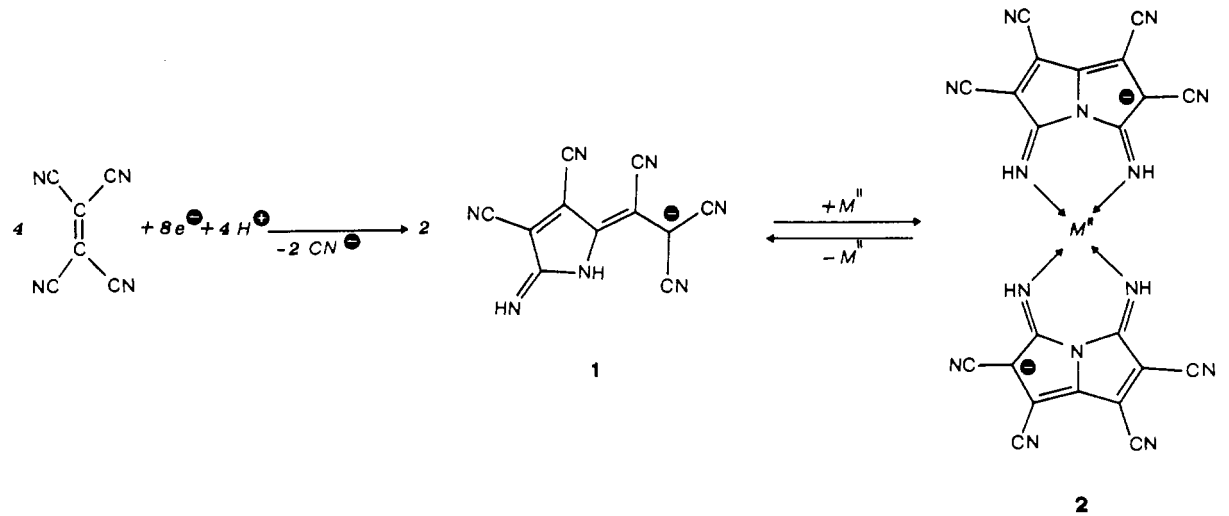

high degree of substitution with cyano groups. In addition, complexes **2** are interesting in that they show an electronic structure very similar to that of the metal phthalocyanines (MPc) (see below) and, like MPc, may be of interest in the fields of molecular metals,[4] special dyes for electrooptical applications,[5] and models for heme proteins.[6]

This paper is concerned with chemical and electrochemical characterization of the Ni(II) complex. The X-ray crystal structures of its adducts with 1,4-dioxane (diox) and water, $Ni(\beta\text{-dtpy})_2{\cdot}2H_2O{\cdot}3diox$ (**3**), and with tetrathiafulvalene (TTF) and tetrahydrofurane (THF), $Ni(\beta\text{-dtpy})_2{\cdot}TTF{\cdot}2THF$ (**4**), are reported.

2. Experimental Section

2.1. General Methods. Microanalyses were by Malissa and Reuter Analytische Laboratorien, Elbach, West Germany, and by Servizio Microanalisi del CNR, Area della Ricerca di Roma.

IR spectra were recorded on a Perkin-Elmer 983 spectrometer on Nujol mulls. The solution electronic spectra were recorded on a Perkin-Elmer 330 spectrometer. A Beckman DK 2A instrument was used to record diffuse reflectance spectra on MgO-diluted samples. Electrical conductivity measurements were performed on polycrystalline samples by using the van de Pauw method with the apparatus described previously.[7] Magnetic measurements were carried out by using the Gouy method at room temperature. Thermal gravimetric analyses (TGA) were performed with a Du Pont 950 apparatus. EPR spectra were obtained with an X-band Varian spectrometer; the magnetic field was measured with a Bruker Model B-NM.20 NMR gaussmeter. XPS spectra were recorded on a VG ESCALAB MK II spectrometer, located at the Servizio ESCA del CNR, Area della Ricerca di Roma. Electrochemical measurements were made under prepurified dinitrogen with an AMEL electrochemistry system (Model 472 polarograph, Model 721 integrator, Model 550 potentiostat) by using a three-electrode configuration in a cell with two compartments separated by a sintered-glass disk (porosity 3). A homemade aqueous SCE electrode was used as a reference (with Luggin capillary) separated from the cell by a salt bridge; in order to minimize liquid–liquid-junction potentials, the procedure reported in the literature[8] was followed. Platinum wire, disk, or guaze was used for the working and counterelectrodes. The solvents (dried, deoxygenated, and freshly distilled) were dimethylformamide (DMF), methanol, and acetone; tetraethylammonium perchlorate (Fluka, dried under vacuum at 60 °C) or Bu_4NBF_4 was used as the supporting electrolyte. For recording EPR spectra during in situ electrolysis, the ESR quartz flat cell (Wildman Model WG-814) was modified into an electrolytic two-compartment cell, the working electrode being a platinum grid located inside the flat section of the cell.

2.2. Materials. A new high-yield procedure has been devised for the large-scale syntheses of the ligand $C_{11}N_7H_2^-$ as the sodium or tetraphenylarsonium salt.[9] The Ni(II) complex as the acetone adduct, $Ni(\beta\text{-dtpy})_2{\cdot}2C_3H_6O$ (**5**), air stable and water free, used as starting material throughout this work, has been made by following the procedure already given;[1] it can also be made by electrolysis at controlled potential, determined by preliminary cyclic voltammetry, using a sacrificial Ni anode, as follows.

2.2.1. Electrosynthesis of 5. Into the anodic compartment of a divided cell with Ni-foil anode (1 × 2 cm) and Pt-wire cathode, filled with 0.04 M $Bu_4N(BF_4)$ in acetone (45 mL) was added 0.020 g of $NaC_{11}N_7H_2$ (7.85×10^{-5} mol). The anode potential was set at 0.900 V (vs SCE), and maintained constant, with an initial current of 1 mA. The color of the solution changed slowly from violet to blue, and after the passage of 12 C, the insoluble **5** separated quantitatively as black microcrystals ($\nu_{acetone}$ = 1675 cm^{-1}).

Suitable crystals for X-ray diffraction studies were grown as dioxane and water adduct, as follows.

2.2.2. Crystal Growth of $Ni(\beta\text{-dtpy})_2{\cdot}2H_2O{\cdot}3diox$ (3). A 1.0-g amount of **5** was dissolved in 100 mL of acetone/water (80/20). The blue solution was filtered, and 30 mL of dioxane was added. On evaporation air-stable purple crystals of **3** separated. Anal. Calcd for $C_{34}H_{32}N_{14}NiO_8$: C, 49.59; H, 3.91; N, 23.81; Ni, 7.13. Found: C, 49.69; H, 3.68; N, 23.14; Ni, 7.10. μ_{eff} = 3.26 μ_B (295 K). ν_{water} = 3640 and 3480 cm^{-1}; ν_{diox} = 760 cm^{-1}.

2.2.3. Synthesis of the TTF Adduct $Ni(\beta\text{-dtpy})_2{\cdot}TTF{\cdot}2THF$ (4). A 0.3-g (0.47-mmol) amount of **5** and 0.192 g (0.94 mmol) of TTF were dissolved in 80 mL of a THF/CH_3CN mixture (40/60), and the mixture was refluxed under N_2. The hot solution was filtered and sealed in a vial. On very slow cooling of the solution from 90 °C to room temperature during 4 days, black crystals of **4** separated. They are moisture sensitive and lose THF when dried.

The elemental analytical data from several analyses are not reproducible due to the partial loss of the solvent when **4** is dried; nevertheless the relative nickel and sulfur contents are in agreement with an atomic ratio Ni/S = 0.25. The compound is diamagnetic. ν_{THF} = 870 cm^{-1}; ν_{TTF} = 792 and 670 cm^{-1}.

2.2.4. Electrosynthesis of $Ni(\beta\text{-dtpy})_2^{\bullet-}NEt_4^+{\cdot}3CH_3OH$ (6). Electrolytic reduction of **5** was carried out in a two-compartment cell with a Pt-disk cathode (3-cm diameter) and a Pt-wire anode under N_2. The cathodic compartment was filled with a solution of **5** (0.5 g, 0.78 mmol) in methanolic 0.08 M $Et_4N(ClO_4)$. The anolyte was methanolic 0.08 M $Et_4N(ClO_4)$. The cathode potential was set at −0.4 V (vs SCE), and maintained constant, with an initial current of 6 mA. Almost immediately after the beginning of electrolysis, a black microcrystalline solid deposited on the cathode surface. Reduction proceeded slowly, and the electrolysis had to be continued for 2 h before the current through the cell became negligible. After the passage of 73.38 C (required charge for the monoreduction of **5**, 75.24 C), the initial blue solution faded and the electrolysis stopped; a quantitative yield of microcrystalline air-sensitive **6** was attained. Anal. Calcd for $C_{33}H_{36}N_{15}NiO_3$: C, 52.89; H, 4.84; N, 28.03; Ni, 7.83; O, 6.40. Found: C, 52.55; H, 4.51; N, 28.82; Ni, 7.52; O, 5.94. μ_{eff} = 1.36 μ_B. The material is a semiconductor: $\sigma = 1.062 \times 10^{-4}$ S cm^{-1}, E_a = 0.024 eV.

(4) (a) Gaudiello, J. C.; Kellog, G. E.; Tetrick, S. M.; Marks, T. J. *J. Am. Chem. Soc.* **1989**, *111*, 5259. (b) Hanack, M.; Deger, S.; Lange, A. *Coord. Chem. Rev.* **1988**, *83*, 115.
(5) Matsuoka, M. *J. Soc. Dyers Colours.* **1989**, *105*, 167.
(6) Kurtz, D. M., Jr. *Chem. Rev.* **1990**, *90*, 585.
(7) Bellitto, C.; Flamini, A.; Gastaldi, L.; Scaramuzza, L. *Inorg. Chem.* **1983**, *22*, 444.
(8) Andruzzi, R.; Trazza, A. *J. Electroanal. Chem. Interfacial Electrochem.* **1978**, *86*, 201.
(9) Flamini, A.; Poli, N. Italian Patent 22867-A/89, 1989.

Table I. Crystal Data and Main Experimental Details for Compounds 3 and 4

	3	4
compd	$Ni(C_{11}N_7H_2)_2 \cdot 2H_2O \cdot 3C_4H_8O_2$	$Ni(C_{11}N_7H_2)_2 \cdot TTF \cdot 2THF$
formula	$C_{34}H_{32}N_{14}NiO_8$	$C_{36}H_{24}N_{14}NiO_2S_4$
fw	823.43	871.6
a, Å	11.184 (3)	11.920 (3)
b, Å	15.682 (4)	21.612 (8)
c, Å	11.720 (4)	7.979 (2)
β, deg	110.77 (2)	109.68 (2)
V, Å^3	1922.0 (9)	1935.4 (9)
Z	2	2
d_{calc}, g cm^{-3}	1.423	1.496
space group	$P2_1/n$	$P2_1/c$
temp, °C	25	25
radiation (λ, Å)	graphite-monochromated Mo Kα (0.71069)	
μ, cm^{-1}	5.792	7.659
transm coeff	0.91–0.95	0.83–0.88
R, %	4.70	4.82
R_w, %	5.00	4.64

In an aprotic solvent (DMF) a similar product is formed but in a lower yield; it contains DMF of crystallization: $Ni(\beta\text{-dtpy})_2^{\bullet-}NEt_4^{+}\cdot 2DMF$. Anal. Calcd for $C_{36}H_{38}N_{17}NiO_2$: C, 54.08; H, 4.79; N, 29.78; Ni, 7.34; O, 4.00. Found: C, 53.20; H, 4.71; N, 29.33; Ni, 7.30; O, 5.63.

2.3. X-ray Crystallography. 2.3.1. Data Collection. A suitable crystal of **3** was fixed by epoxy resin on a glass fiber and mounted on a Nicolet $P2_1$ diffractometer. Since crystals of **4** were moisture sensitive, a single crystal was embedded by silicone grease in a glass capillary in the presence of mother liquor. Preliminary oscillating and Weissenberg photographs indicated monoclinic symmetry for both compounds. Systematic absences were consistent with space group $P2_1/n$ for **3** and $P2_1/c$ for **4**. Data for the two compounds have been collected by following essentially the same procedure. Unit cell parameters and their standard deviations were derived from the setting angles of 25 automatically centered reflections. Only random fluctuations (<3%) were observed in the intensity of two standard reflections during the course of data collection for compound **3**, while for **4** a systematic decay reduced their intensities to 65% of the initial values. Data were corrected for Lorentz and polarization factors (and for decay effect in the case of **4**). No correction for absorption was included because of the small size of the crystals and the small values of μ. Furthermore, a ψ scan around the scattering vector of selected reflections showed no significant deviation.

A summary of the main crystal data for both compounds and details of data collection are given in Table I.

2.3.2. Solution and Refinement of the Structures. Both structures were solved by conventional Patterson and Fourier methods and refined by full-matrix least-squares methods. The final refinements were made with anisotropic temperature factors for the non-hydrogen atoms; hydrogens, excluded those belonging to the water molecule in **3**, were placed in their geometrical calculated positions and restrained to ride on their associated carbon or nitrogen atoms.

The quantity minimized was $\sum w(|F_o| - |F_c|)^2$, where $w = 1/[\sigma(F_o)]^2$.

Residual R and R_w indices, defined as $R = \sum||F_o| - |F_c||/\sum|F_o|$ and $R_w = [\sum w(|F_o| - |F_c|)^2/\sum w(F_o)^2]^{1/2}$, were $R = 0.047$ and $R_w = 0.050$ for **3** and $R = 0.048$ and $R_w = 0.046$ for **4**.

Neutral scattering factors, f' and f'' values, were those from the literature.[10] All calculations were carried out by using the SIR-CAOS Crystallographic Program System[11] running on a DG Eclipse/8000 II computer. Final atomic positional parameters for non-hydrogen atoms and their U_{eq} values (Å^2) are given in Tables II and III.

3. Results and Discussion

3.1. Characterization of the Nickel Complexes 3 and 5. 3.1.1. Syntheses and Chemicophysical Properties. As reported in Scheme I, like the other metal(II) complexes **2**, a Ni(II) complex results from a reductive condensation of four TCNE molecules to two β-diimino anions around the metal center; we emphasize the importance of this reaction: it is reminiscent of the formation reaction of MPc, deriving from the reductive cyclotetramerization of four 1,2-dicyanobenzene molecules; the two systems have very similar electronic properties too (see below).

The Ni complex is formed in either aqueous or anhydrous solvents; in either case a large excess of Ni(II) ion is needed; it incorporates oxygenated solvent of crystallization and is hexacoordinated in the solid state; on heating, **3** and **5** lose the solvent almost completely as shown by TGA measurements: **5** shows a

Table II. Atomic Coordinates and Equivalent Isotropic Thermal Parameters, with Their Esd's in Parentheses, for the Non-Hydrogen Atoms of Compound 3

	x	y	z	U(eq),[a] Å^2
Ni(1)	0.0000	0.0000	0.0000	0.0306 (3)
N(1)	−0.0867 (4)	−0.0589 (3)	0.2264 (4)	0.038 (2)
C(2)	−0.0580 (5)	−0.1274 (3)	0.1646 (4)	0.033 (2)
C(3)	−0.0793 (5)	−0.2011 (3)	0.2311 (5)	0.035 (2)
C(4)	−0.1203 (5)	−0.1731 (3)	0.3233 (5)	0.038 (2)
C(5)	−0.1231 (5)	−0.0842 (3)	0.3228 (5)	0.040 (2)
C(6)	−0.1479 (4)	−0.0095 (4)	0.3766 (4)	0.041 (2)
C(7)	−0.1265 (5)	0.0599 (4)	0.3111 (5)	0.037 (2)
N(8)	−0.0222 (4)	−0.1161 (2)	0.0737 (4)	0.033 (2)
C(9)	−0.0595 (5)	−0.2873 (4)	0.2036 (5)	0.043 (2)
C(10)	−0.1595 (5)	−0.2261 (4)	0.4053 (5)	0.045 (2)
C(11)	−0.1802 (5)	−0.0080 (4)	0.4835 (5)	0.047 (2)
C(12)	−0.1287 (6)	0.1479 (4)	0.3412 (5)	0.046 (3)
C(13)	−0.0886 (5)	0.0298 (3)	0.2107 (5)	0.033 (2)
N(14)	−0.0612 (4)	0.0640 (3)	0.1249 (4)	0.036 (2)
N(15)	−0.0436 (6)	−0.3562 (3)	0.1828 (5)	0.076 (3)
N(16)	−0.1941 (5)	−0.2672 (3)	0.4667 (5)	0.065 (2)
N(17)	−0.2024 (5)	−0.0086 (4)	0.5704 (4)	0.079 (3)
N(18)	−0.1278 (5)	0.2175 (3)	0.3661 (5)	0.067 (3)
Ow	0.1928 (3)	0.0135 (2)	0.1216 (3)	0.042 (1)
O(101)	0.0211 (4)	0.2484 (2)	0.1014 (4)	0.056 (2)
C(102)	0.1282 (6)	0.2338 (4)	0.2086 (6)	0.069 (3)
C(103)	0.2294 (6)	0.2993 (5)	0.2252 (7)	0.083 (4)
O(104)	0.1797 (5)	0.3817 (3)	0.2291 (4)	0.073 (2)
C(105)	0.0737 (7)	0.3982 (4)	0.1207 (6)	0.075 (3)
C(106)	−0.0271 (6)	0.3331 (4)	0.1034 (6)	0.066 (3)
O(201)	0.3818 (4)	0.0059 (3)	0.0163 (4)	0.070 (2)
C(202)	0.4382 (7)	0.0782 (4)	−0.0149 (7)	0.076 (4)
C(203)	0.5203 (7)	0.0524 (5)	−0.0851 (7)	0.086 (4)

[a] $U(\text{eq}) = (1/3)\sum_i\sum_j U_{ij}a^*_i a^*_j \vec{a}_i \vec{a}_j$.

Table III. Atomic Coordinates and Equivalent Isotropic Thermal Parameters, with Their Esd's in Parentheses, for the Non-Hydrogen Atoms of Compound 4

	x	y	z	U(eq),[a] Å^2
Ni(1)	0.0000	0.0000	0.0000	0.0434 (3)
N(1)	−0.2095 (3)	0.0841 (1)	−0.2266 (4)	0.044 (1)
C(2)	−0.2459 (3)	0.0306 (2)	−0.1695 (5)	0.042 (1)
C(3)	−0.3746 (3)	0.0343 (2)	−0.2415 (5)	0.046 (2)
C(4)	−0.4056 (3)	0.0891 (2)	−0.3414 (5)	0.048 (2)
C(5)	−0.3017 (4)	0.1205 (2)	−0.3326 (5)	0.047 (2)
C(6)	−0.2474 (4)	0.1705 (2)	−0.3833 (5)	0.049 (2)
C(7)	−0.1236 (4)	0.1638 (2)	−0.3094 (5)	0.048 (2)
N(8)	−0.1685 (3)	−0.0087 (2)	−0.0749 (4)	0.047 (1)
C(9)	−0.4564 (4)	−0.0100 (2)	−0.2179 (6)	0.055 (2)
C(10)	−0.5252 (4)	0.1077 (2)	−0.4372 (6)	0.061 (2)
C(11)	−0.3044 (4)	0.2214 (2)	−0.4921 (6)	0.064 (2)
C(12)	−0.0392 (4)	0.2060 (2)	−0.3302 (6)	0.057 (2)
C(13)	−0.0987 (4)	0.1068 (2)	−0.2089 (5)	0.043 (2)
N(14)	−0.0046 (3)	0.0763 (1)	−0.1186 (4)	0.047 (1)
N(15)	−0.5241 (4)	−0.0445 (2)	−0.2025 (6)	0.081 (2)
N(16)	−0.6216 (4)	0.1205 (2)	−0.5122 (6)	0.094 (2)
N(17)	−0.3449 (4)	0.2623 (2)	−0.5799 (7)	0.103 (3)
N(18)	0.0249 (4)	0.2416 (2)	−0.3518 (7)	0.089 (2)
C(101)	0.0314 (4)	−0.0232 (2)	0.5499 (5)	0.053 (2)
S(102)	0.1883 (1)	−0.0256 (1)	0.6276 (2)	0.066 (1)
C(103)	0.1979 (5)	−0.0935 (2)	0.7455 (6)	0.069 (2)
C(104)	0.0985 (5)	−0.1213 (2)	0.7394 (6)	0.071 (2)
S(105)	−0.0354 (1)	−0.0871 (1)	0.6141 (2)	0.071 (1)
O(201)	0.2285 (3)	0.1260 (1)	−0.0469 (4)	0.068 (1)
C(202)	0.2955 (5)	0.1312 (3)	−0.1622 (7)	0.085 (3)
C(203)	0.3981 (6)	0.1713 (4)	−0.078 (1)	0.123 (4)
C(204)	0.3685 (8)	0.2026 (4)	0.057 (1)	0.18 (1)
C(205)	0.2562 (6)	0.1791 (3)	0.0700 (8)	0.100 (3)

[a] See footnote *a* of Table II.

(10) *International Tables for X-ray Crystallography*; Kynoch Press: Birmingham, England, 1974; Vol. IV.
(11) Camalli, M.; Capitani, D.; Cascarano, G.; Cerrini, S.; Giacovazzo, C.; Spagna, R. Italian Patent 35403c/86, 1986.

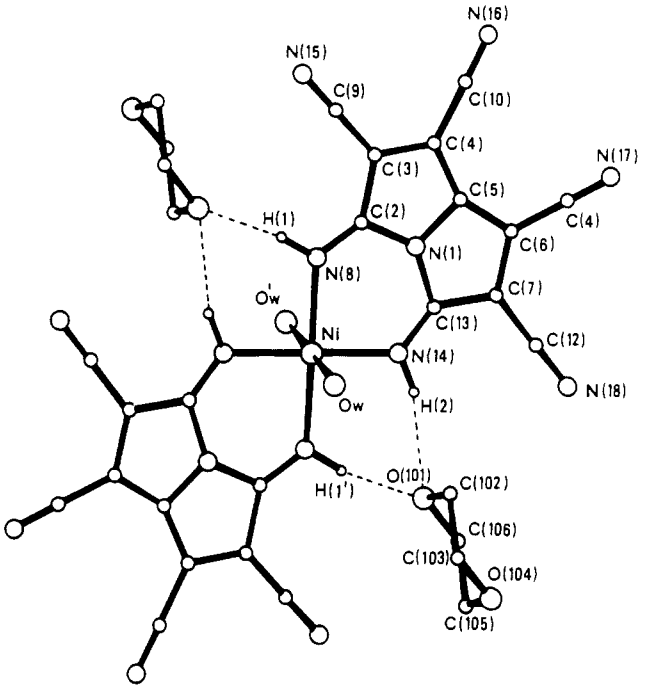

Figure 1. Labeling scheme and perspective view of $Ni(C_{11}N_7H_2)_2 \cdot 2H_2O \cdot 3C_4H_8O_2$ (**3**), showing the nickel complex ligand system, the apical water molecules, and the unconstrained, imino–hydrogen-bonded dioxane molecules.

loss of 16.8% (204 °C) (theoretical amount for two acetone molecules, 18.1%); **3** shows a loss of 30.7% (60–290 °C) (theoretical amount for three dioxane and two water molecules, 34.0%); on heating at higher temperature (≈350 °C) under vacuum (10^{-3} mmHg), they do not sublime but decompose, releasing the free percyano acid $C_{11}N_7H_3$ (S = acetone, water, dioxane):

$$Ni(C_{11}N_7H_2)_2 \cdot S \xrightarrow{-S} Ni(C_{11}N_7H_2)_2 \rightarrow C_{11}N_7H_3$$

$Ni(\beta\text{-dtpy})_2 \cdot S$ compounds are soluble in polar solvents: DMF > $CH_3OH \approx C_2H_5OH$ > acetone > CH_3CN > THF (solubilities in alcohols, $\approx 10^{-3}$ M, independent of S, which rapidly exchanges). Both acids and bases decompose them. In solution they do not obey Beer's law, because of dissociation to the free pyrrolinine anion **1**; the dissociation constant depends on the solvent in the order DMF > CH_3CN > alcohols; the dissociation rate is low in DMF so that the modification of the absorption spectrum in this solvent can be observed in time with one isosbestic point at 612 nm. An excess of Ni(II) ion reverses the dissociation completely.

3.1.2. Crystal Structure of 3. The structure of $[Ni(\beta\text{-dtpy})_2 \cdot 2H_2O] \cdot 3$diox (**3**) consists of well-separated centrosymmetrical complex units, adducted with two water molecules and connected, via a three-dimensional net of hydrogen bonds, by three dioxane molecules (Figures 1 and 2). The nickel atom, located at the unit cell origin, is six-coordinated in an octahedral geometry NiN_4O_2 with only a slight tetragonal distortion, the mean Ni–N equatorial distances being 2.075 (4) Å vs the Ni–O apical one of 2.132 (4) Å. Such values are comparable with literature data[12] and similar to those found in the analogous $Ni(\beta\text{-dtpy})_2 \cdot 2THF \cdot 2THF$ (**7**),[13] in which the oxygen atoms derive from two THF molecules in the apical positions, and the coordination distances are Ni–N = 2.06 Å and Ni–O = 2.16 Å.

The $Ni(\beta\text{-dtpy})_2$ complex unit is almost planar, with a mean deviation from the least-squares best plane of 0.2 Å for the pe-

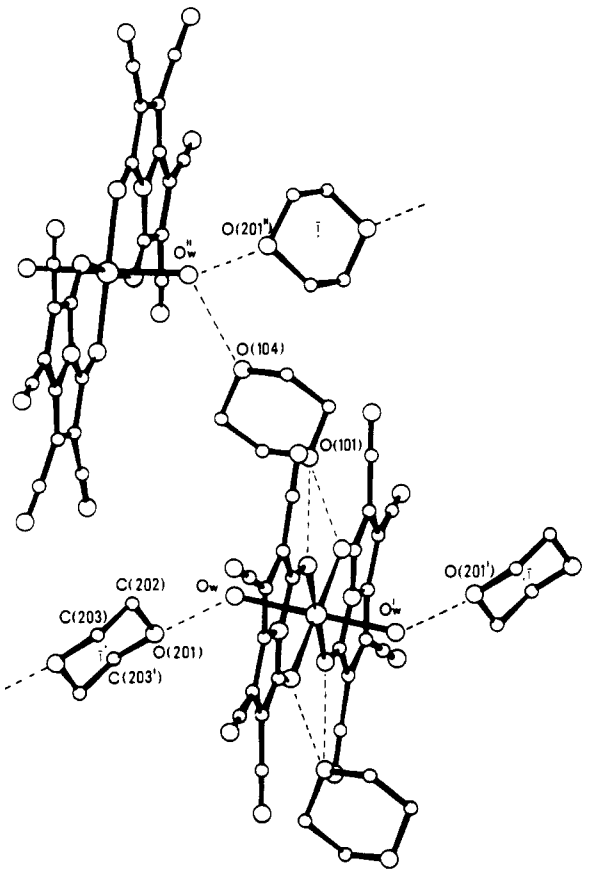

Figure 2. Main interactions and packing of compound **3**, with the labeling scheme of the constrained (centrosymmetrical) dioxane molecule. Equivalent positions: I, $-x, -y, -z$; II, $^1/_2 - x, y - ^1/_2, ^1/_2 - z$.

Table IV. Bond Lengths (Å) and Angles (deg), with Esd's in Parentheses, within the Nickel Complex Macrocyclic System for Compound **3**[a]

Ni(1)–N(8)	2.068 (4)	C(4)–C(10)	1.451 (8)
Ni(1)–N(14)	2.081 (4)	C(5)–C(6)	1.405 (8)
Ni(1)–Ow	2.132 (4)	C(6)–C(7)	1.400 (8)
N(1)–C(2)	1.395 (6)	C(6)–C(11)	1.421 (7)
N(1)–C(5)	1.388 (7)	C(7)–C(12)	1.427 (8)
N(1)–C(13)	1.402 (6)	C(7)–C(13)	1.463 (7)
C(2)–C(3)	1.461 (7)	C(9)–N(15)	1.136 (7)
C(2)–N(8)	1.276 (6)	C(10)–N(16)	1.131 (7)
C(3)–C(4)	1.387 (7)	C(11)–N(17)	1.131 (7)
C(3)–C(9)	1.425 (7)	C(12)–N(18)	1.129 (8)
C(4)–C(5)	1.393 (8)	C(13)–N(14)	1.270 (6)
N(14)–Ni(1)–N(8)	90.7 (1)	C(6)–C(5)–C(4)	147.2 (5)
Ow–Ni(1)–N(8)	92.9 (2)	C(7)–C(6)–C(5)	107.7 (4)
Ow–Ni(1)–N(14)	89.4 (2)	C(11)–C(6)–C(5)	124.1 (5)
C(5)–N(1)–C(2)	113.0 (4)	C(11)–C(6)–C(7)	128.1 (5)
C(13)–N(1)–C(2)	133.7 (4)	C(12)–C(7)–C(6)	126.5 (5)
C(13)–N(1)–C(5)	113.2 (4)	C(13)–C(7)–C(6)	110.1 (5)
C(3)–C(2)–N(1)	102.7 (4)	C(13)–C(7)–C(12)	123.2 (5)
N(8)–C(2)–N(1)	121.7 (4)	C(2)–N(8)–Ni(1)	126.2 (3)
N(8)–C(2)–C(3)	135.6 (4)	N(15)–C(9)–C(3)	179.3 (6)
C(4)–C(3)–C(2)	109.0 (4)	N(16)–C(10)–C(4)	177.8 (8)
C(9)–C(3)–C(2)	124.2 (4)	N(17)–C(11)–C(6)	177.7 (7)
C(9)–C(3)–C(4)	126.8 (5)	N(18)–C(12)–C(7)	178.6 (8)
C(5)–C(4)–C(3)	109.1 (5)	C(7)–C(13)–N(1)	102.2 (4)
C(10)–C(4)–C(3)	126.5 (5)	N(14)–C(13)–N(1)	121.8 (5)
C(10)–C(4)–C(5)	124.3 (5)	N(14)–C(13)–C(7)	136.0 (5)
C(4)–C(5)–N(1)	106.1 (4)	C(13)–N(14)–Ni(1)	125.8 (3)
C(6)–C(5)–N(1)	106.7 (4)		

[a] Geometrical and conformational parameters of the dioxane molecules are reported as supplementary material.

(12) (a) Suh, M. P.; Choi, J.; Kang, S. G.; Shin, W. *Inorg. Chem.* **1989**, *28*, 1763. (b) Newkome, G. R.; Gupta, V. G.; Fronczek, F. R.; Pappalardo, S. *Inorg. Chem.* **1984**, *23*, 2400. (c) Loeb, S. J.; Stephan, D. W.; Willis, C. J. *Inorg. Chem.* **1984**, *23*, 1509.

(13) Preliminary crystallographic information on **7**: space group $P\bar{1}$; unit cell dimensions a = 9.884 (3) Å, b = 10.887 (3) Å, c = 11.725 (4) Å, α = 97.84 (2)°, β = 111.02 (2)°, γ = 112.45 (2)°. Of the four THF molecules, two are apically oxygen coordinated to the nickel atom; the other two are laterally adducted via hydrogen bonds to the imino groups, as in compound **4**.

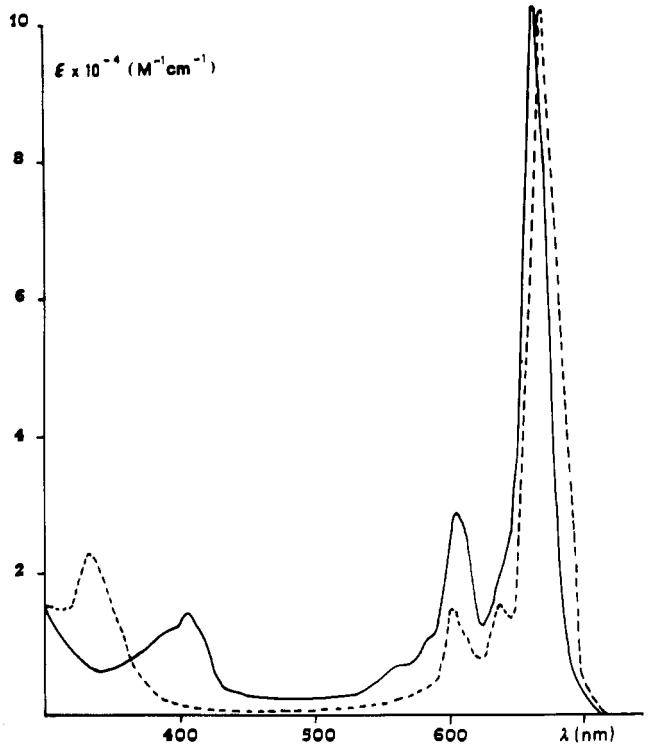

Figure 3. Solution electronic spectra of NiPc (---) (1,2,4-trichlorobenzene) and of Ni(β-dtpy)$_2$ (—) (methanol/water (5/1) + 0.2 M $NiCl_2 \cdot 6H_2O$).

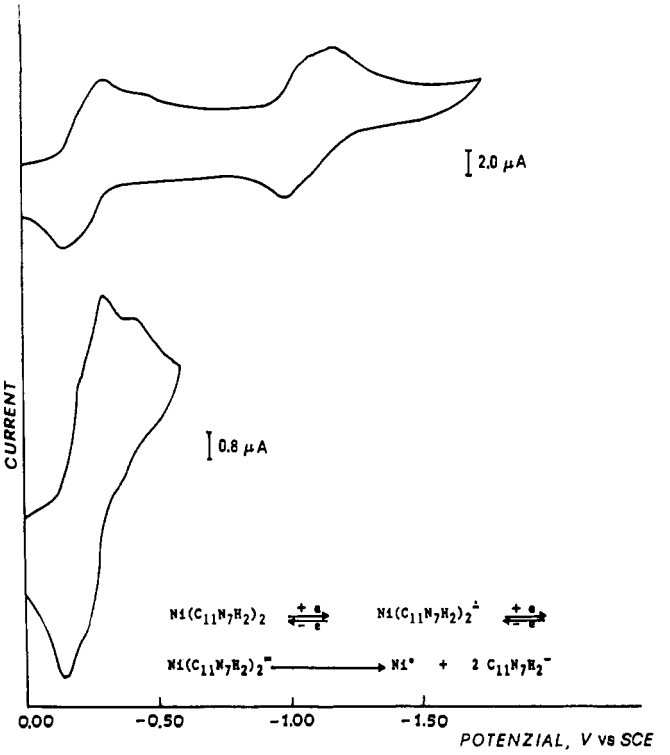

Figure 4. Cyclic voltammetry of Ni(β-dtpy)$_2$ (1 mM) at a platinum electrode in DMF with 0.1 M Et_4NClO_4 (scan rate 200 mV/s).

ripheral cyano groups but only 0.02 Å for the internal atoms.

Interatomic distances and angles, reported in Table IV, fall in the range typical for sp^2 C–C and C–N values[14] and are consistent with a localized imino C=NH double bond (1.273 Å) and with a delocalized charge only over the external C(3)–C(7) atoms, while the central N(1) atom is involved in essentially single bonds with its neighboring carbon atoms (mean value 1.394 Å) as found in similar heterocyclic fused system.[15]

Two crystallographically nonequivalent 1,4-dioxane molecules are present. Both of them act as bridging groups between equivalent metal complex units. The first one, O(101)–C(106), almost orthogonal to the Ni(β-dtpy)$_2$ plane, interacts[16] via O(101) with imino hydrogens (Figure 1) distances O(101)···H(1′) = 2.019 (6) Å and O(101)···H(2) = 2.225 (6) Å (sum of van der Waals radii 2.70 Å) and via O(104) with the nickel-coordinated water molecule (O(104)···Ow″ = 2.757 (5) Å) (Figure 2).

The second one, O(201)–C(203′) placed at $^1/_2$, 0, 0 and 0, $^1/_2$, $^1/_2$ symmetry centers, links only water molecules O(201)···Ow = 2.803 (5) Å by means of hydrogen bonds within a zigzag sequence O(201)···Ow–Ni–Ow′···O(201′)··· running along the *x* direction.

Geometrical and conformational parameters of the two dioxane molecules, comparable with literature data,[17] are reported as supplementary material.

3.1.3. Electronic Spectra. The absorption solution spectrum of the undissociated $Ni(C_{11}N_7H_2)_2$ is reported in Figure 3, together with that of NiPc for comparison. They are amazingly alike; for example, the extinction coefficients of the most intense peak of the Q band are as follows: 103 000, $Ni(C_{11}N_7H_2)_2$; 102 000 (lit. value 100 000),[18] NiPc. Obviously very similar π-ligand orbitals must be involved in the electronic transitions of both systems, although the two systems differ in their degree of conjugation, symmetry (D_{4h} and D_{2h}), and number of π orbitals (16 and 18) and π electrons (18 and 20). A satisfactory explanation will therefore require a theoretical treatment, such as the one made by Gouterman and co-workers on MPc,[19] extended to this system.

Moreover, the reflectance spectra show additional bands at 10.26×10^3 cm^{-1} in **3** and 8.9×10^3 cm^{-1} in **5**, absent in solution, arising from d–d transitions confined into the tetragonally distorted octahedral Ni(II) chromophore.

Scheme II

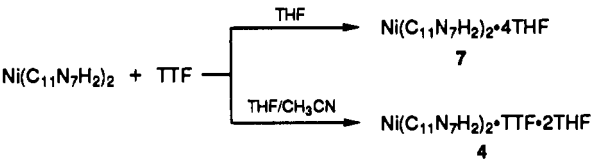

3.1.4. Electrochemical Behavior. Cyclic voltammograms of **5** are shown in Figure 4. Only reduction waves are observed. At least three electrons are consumed by $Ni(C_{11}N_7H_2)_2$ from −0.2 to −0.5 V vs SCE (−0.22, −0.31, −0.42), and they originate from the first wave; this is not reversible as a whole ($i_e/i_a > 1$; $\Delta E > 0.1$; the reduction potentials are dependent on the scan rate, $E/(\Delta E/t) = 0.2$ s). From the coulometry it results that the first electron transfer is reversible (see below) but not the second one, since the dianion decomposes rapidly, in the electrolysis time scale, into the metal and the pyrrolenine anion **1**.[20]

The radical monoanion $Ni(C_{11}N_7H_2)_2^{\bullet-}$ is not very stable in solution even under dinitrogen; it disproportionates into the corresponding neutral and dianion species. Consequently, only a very small stationary concentration of $Ni(C_{11}N_7H_2)_2^{\bullet-}$ can be generated in solution. In fact EPR spectra of **5**, recorded during in situ electrolysis in DMF with $LiClO_4$ as the supporting electrolyte, reveal an unresolved structure signal ($g = 2.0057$) in-

(14) (a) Stam, C. H.; Counotte-Potman, A. D.; Plas, H. C. *J. Org. Chem.* **1982**, *47*, 2856. (b) Burke-Laing, M.; Laing, M. *Acta Crystallogr., Sect. B* **1976**, *32*, 3216.
(15) (a) Hosmane, R. S.; Rossman, M. A.; Leonard, N. J. *J. Am. Chem. Soc.* **1982**, *104*, 5497. (b) Murray-Rust, M.; Murray-Rust, J.; Scopes, D. I. C.; Oxford, A. W. *Acta. Crystallogr.* **1982**, *B38*, 2694.
(16) Taylor, R.; Kennard, O. *J. Am. Chem. Soc.* **1982**, *104*, 5063.
(17) Foces-Foces, C.; Cano, F. H. *Tetrahedron* **1988**, *44*, 5117.
(18) Barret, G. M. A.; Broderick, W. E.; Hoffmann, B. M.; Velasquez, C. S. *J. Org. Chem.* **1989**, *54*, 3233.
(19) Schaffer, A. M.; Gouterman, M. *Theoret. Chim. Acta* **1972**, *25*, 62.
(20) A controlled-potential reduction of the bulk solution at −0.3 V (vs SCE), in CH_3OH with $LiClO_4$ as supporting electrolyte, requires approximately two electrons/mol, and the visible spectrum of the resulting violet solution reveals the presence of a stoichiometric amount of **1**, according to the scheme reported in Figure 4.

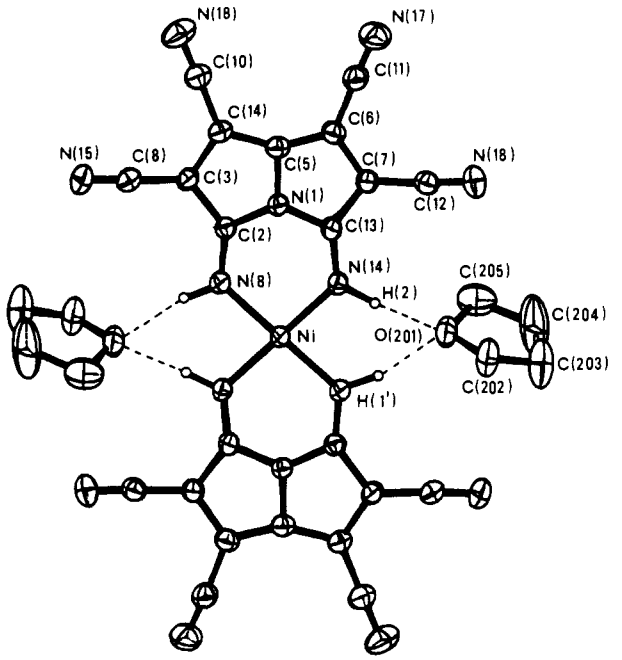

Figure 5. Perspective drawing and numbering scheme of $Ni(C_{11}N_7H_2)_2$·TTF·2THF (**4**), showing the square-planar nickel complex and imino–hydrogen-bonded tetrahydrofuran molecules. Thermal ellipsoids are at the 30% probability level.

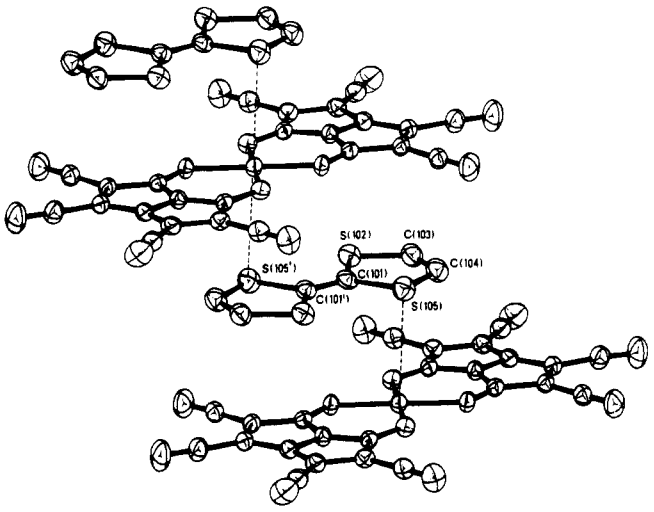

Figure 6. View of compound **4**, showing the mixed, slipped stack of the nickel complex and TTF units (with TTF labeling scheme). Equivalent positions: I, $-x, -y, 1-z$.

creasing slowly from zero to a low constant value only in the very first period. Nevertheless, the anion radical $Ni(\beta\text{-dtpy})_2^{\bullet-}$ can be quantitatively isolated, as $Ni(\beta\text{-dtpy})_2^{\bullet-}Et_4N^+$, when the controlled-potential reduction of the bulk solution is carried out in methanol with Et_4NClO_4 as the supporting electrolyte (see below).

3.2. Interaction with TTF. The interaction with TTF is weak, and the charge-transfer complex **4** can be obtained only from a solution of a THF/CH_3CN mixture as solvent (Scheme II). In pure THF complex **7** is formed, for which preliminary structure information has been given above.[13]

3.2.1. X-ray Crystal Structure of 4. The crystal structure of $Ni(\beta\text{-dtpy})_2$·TTF·2THF (**4**) reflects the solid-state cooperative interactions evidenced by the reflectance spectrum.

It can best be described as slipped-stacked alternate units of Ni complex and TTF^0 molecules. The nickel atom, in a square-planar arrangement within the ligand plane (Figure 5), interacts apically with two sulfur atoms from two TTF units, at a distance of 3.51 Å (Figure 6). The displacement of the molecular centers of the two components may be the result of a specific interaction between the sulfur of the donor and the nickel of the acceptor. The stack runs along the short *c* axis, the TTF molecule being located on the symmetry center at 0, 0, $^1/_2$. The TTF and complex planes are orthogonal to the *bc* plane and form an angle of 60° with the *z* direction.

Also a $\pi-\pi$ interaction between the complex and TTF units can be invoked,[21] given the degree of superposition and the interplanar distance of 3.46 Å observed.

Interatomic distances and angles of **4** are reported in Table V. The Ni–N coordination distance of 1.897 (3) Å is strictly comparable with the one found in the nickel phthalocyaninato NiPcI of 1.887 (6) Å[22] or in other analogous NiN_4 square-planar complexes.[23,24]

Table V. Bond Lengths (Å) and Angles (deg), with Esd's in Parentheses, for Compound **4**

Ni(1)–N(8)	1.902 (3)	C(9)–N(15)	1.135 (6)
Ni(1)–N(14)	1.893 (3)	C(10)–N(16)	1.136 (8)
N(1)–C(2)	1.366 (5)	C(11)–N(17)	1.130 (8)
N(1)–C(5)	1.384 (6)	C(12)–N(18)	1.137 (6)
N(1)–C(13)	1.370 (5)	C(13)–N(14)	1.291 (6)
C(2)–C(3)	1.448 (6)	C(101)–S(102)	1.762 (5)
C(2)–N(8)	1.293 (6)	C(101)–S(105)	1.754 (4)
C(3)–C(4)	1.406 (6)	S(102)–C(103)	1.725 (5)
C(3)–C(9)	1.423 (6)	C(103)–C(104)	1.315 (8)
C(4)–C(5)	1.393 (6)	C(104)–S(105)	1.738 (6)
C(4)–C(10)	1.430 (7)	O(201)–C(202)	1.411 (6)
C(5)–C(6)	1.388 (5)	O(201)–C(205)	1.444 (7)
C(6)–C(7)	1.400 (7)	C(202)–C(203)	1.46 (1)
C(6)–C(11)	1.425 (7)	C(203)–C(204)	1.41 (1)
C(7)–C(12)	1.408 (6)	C(204)–C(205)	1.47 (1)
C(7)–C(13)	1.445 (6)	C(101)–C(101')	1.339 (8)

N(14)–Ni(1)–N(8)	94.5 (1)	C(13)–C(7)–C(12)	126.5 (4)
C(5)–N(1)–C(2)	114.1 (3)	C(2)–N(8)–Ni(1)	126.0 (3)
C(13)–N(1)–C(2)	132.2 (4)	N(15)–C(9)–C(3)	178.1 (6)
C(13)–N(1)–C(5)	113.5 (3)	N(16)–C(10)–C(4)	177.7 (5)
C(3)–C(2)–N(1)	103.6 (4)	N(17)–C(11)–C(6)	176.8 (5)
N(8)–C(2)–N(1)	120.4 (4)	N(18)–C(12)–C(7)	176.9 (6)
N(8)–C(2)–C(3)	136.0 (4)	C(7)–C(13)–N(1)	103.8 (4)
C(4)–C(3)–C(2)	108.2 (3)	N(14)–C(13)–N(1)	120.0 (3)
C(9)–C(3)–C(2)	126.3 (4)	N(14)–C(13)–C(7)	136.2 (4)
C(9)–C(3)–C(4)	125.5 (4)	C(13)–N(14)–Ni(1)	126.7 (3)
C(5)–C(4)–C(3)	108.8 (4)	S(105)–C(101)–S(102)	113.9 (3)
C(10)–C(4)–C(3)	124.3 (4)	C(103)–S(102)–C(101)	94.9 (2)
C(10)–C(4)–C(5)	126.9 (4)	C(104)–C(103)–S(102)	118.4 (5)
C(4)–C(5)–N(1)	105.3 (3)	S(105)–C(104)–C(103)	117.8 (4)
C(6)–C(5)–N(1)	105.5 (4)	C(104)–S(105)–C(101)	94.9 (2)
C(6)–C(5)–C(4)	149.1 (5)	C(205)–O(201)–C(202)	107.5 (4)
C(7)–C(6)–C(5)	109.1 (4)	C(203)–C(202)–O(201)	108.4 (5)
C(11)–C(6)–C(5)	127.2 (4)	C(204)–C(203)–C(202)	104.5 (6)
C(11)–C(6)–C(7)	123.7 (4)	C(205)–C(204)–C(203)	110.8 (8)
C(12)–C(7)–C(6)	125.3 (4)	C(204)–C(205)–O(201)	104.2 (5)
C(13)–C(7)–C(6)	108.1 (4)		

Table VI. Mean Interatomic Distances in the Macrocyclic Ligand System of Compounds **3**, **4**, and $Cu(\beta\text{-dtpy})_2$·2THF (**8**)

	3	**4**	**8**
metal	Ni, d^8	Ni, d^8	Cu, d^9
coord geom	octahedral	sq planar	tetrag-dist octahedral
inner params			
M–N	2.075 (3)	1.897 (3)	1.989 (5)
C=NH	1.273 (6)	1.293 (6)	1.287 (8)
N(1)–C(2), N(1)–C(13)	1.397 (6)	1.370 (6)	1.377 (8)
C(2)–C(3), C(7)–C(13)	1.463 (6)	1.448 (6)	1.448 (9)
peripheral params			
N(1)–C(5)	1.387 (6)	1.383 (6)	1.375 (9)
C(3)–C(4), C(6)–C(7)	1.392 (7)	1.403 (7)	1.402 (9)
C(4)–C(5), C(5)–C(6)	1.398 (7)	1.390 (6)	1.393 (9)

(21) Herbstein, F. H. *Perspect. Struct. Chem.* **1971**, *4*, 166.
(22) Schramm, C. J.; Scaringe, R. P.; Stojakovic, D. R.; Hoffman, B. M.; Ibers, J. A.; Marks, T. J. *J. Am. Chem. Soc.* **1980**, *102*, 6702.

Table VII. Nitrogen and Nickel Binding Energies (eV)[a] and N/Ni Atomic Ratios[b] (in Parentheses) from XPS Spectra of Compounds **3** and **6**

	N_{1s}				
sample	–C≡N	N<	=N–H	$^+NEt_4$	$Ni_{2P_{3/2}}$
3	398.6 (8.2)	399.6 (2.0)	401.0 (4.1)		855.6 (1.0)
6	398.6 (8.3)	399.6 (2.1)	401.0 (4.0)	402.0 (1.1)	855.4 (1.0)

[a] Referenced to the C_{1s} pump-oil hydrocarbon peak (285.0 eV). [b] According to the procedures proposed by Wagner.[31]

A comparison of bond length values in the ligand systems of compounds **3** and **4**, and of Cu(β-dtpy)$_2$·2THF (**8**),[1] is made in Table VI.

Apart from the expected decrease in bond lengths involving nickel on going from high-spin, octahedral to low-spin, square-planar geometry, a slight influence of the metal coordination geometry on the electronic distribution (and related bond distances) within the "inner" part of the heterocyclic system can be noted.

Bond lengths of the TTF unit can be compared with the theoretical ones calculated as a function of the fractional charge[25] and with the ones found in several compounds containing TTF^0 and/or $TTF^{\bullet+}$.[26] In our case the TTF neutral character is clearly confirmed by its bond distances and angles in the whole.

The high thermal parameters associated with the THF atoms are due essentially to the conformational disorder between the twist and envelope forms of the pentaatomic THF ring molecule.[27,28] Its least-squares mean plane is almost orthogonal to the nickel complex plane: two THF units, laterally adducted with formation of NH···O(THF) hydrogen bonds O(201)···H(2) = 1.786 (5) Å, and O(201)···H(1′) = 1.825 (5) Å, so play the role of dioxane in compound **3**.

3.2.2. Properties of 4. This is a charge-transfer complex, and its IR spectrum is essentially a composite of **7** and TTF. In solution it is almost completely dissociated and the charge-transfer transition, due to discrete pairs of single donor and acceptor molecules, appears as a weak shoulder at 760 nm, which increases with TTF concentration. In the solid state the infinite stacks of alternate donor and acceptor molecules originate the broad an very intense low-energy band at 1200 nm in the reflectance spectrum.

3.3. Properties of 6. This is a radical-anion salt, stable in the solid state, which can be formed only when the potentiostatically controlled electrolysis of **5** is carried out in the presence of a large excess of Et_4N^+ cation in methanol, where **6** is completely insoluble; after the passage of one electron/mol, the electrolysis stops and **6** sticks firmly to the platinum-disk cathode; one electron reoxidation makes it dissolve, regenerating more than 95% of the original visible spectrum; **6** can also be oxidized quantitatively back to **5** by Wudl's salt. Unfortunately, **6** decomposes in solution even under dinitrogen, because of the tendency of the radical-monoanion Ni(β-dtpy)$_2^{\bullet-}$ to disproportionate, preventing us from obtaining good quality crystals for an X-ray diffraction study. Nevertheless, a structure consisting of segregated cations and anion stacks can be inferred from its electrical, magnetic, and optical properties.

It is a semiconductor ($\sigma_{RT} = 1.062 \times 10^{-4}$ S cm^{-1}, exponentially temperature dependent from 77 to 300 K) with a low activation energy for conduction ($E_a = 0.024$ eV according to $\sigma = \sigma_0 \exp(-(E/(RT)))$, similar to the simple 1/1 $TCNQ^{\bullet-}$ salts of cations of low electrophilicity belonging to class I of Torrance's classification, but different in conductivity by a factor of 10^5 from that of the most pertinent class I typical example, i.e., $Et_3NH^+TCNQ^{\bullet-}$ (**9**) ($\sigma = 10^{-9}$ S cm^{-1});[29] on-site Coulombic repulsion in **6** is smaller than that in **9** as accounted for by the differences between the first and the second reduction potentials ($\Delta E = E_1 - E_2$) in the acceptors (Ni(β-dtpy)$_2$, $\Delta E \approx 0.09$ V; TCNQ, $\Delta E = 0.46$ V[30]).

The magnitude of μ at room temperature (1.36 μ_B) is lower than the expected value per Ni(β-dtpy)$_2^{\bullet-}$ unit, thus indicating a partial antiferromagnetic coupling of the unpaired electrons along the anion stacks.

In the reflectance spectrum it shows a broad band, absent in **5**, with the maximum at 1000 nm, originated by a charge-transfer transition between adjacent molecules in the stacking direction; the low-energy tail of this electronic absorption obscures the IR N–H and O–H stretching bands.

As far as the delocalization of the odd electron in the radical-monoanion Ni(β-dtpy)$_2^{\bullet-}$ is concerned, both ESR and ESCA data of **6** show conclusively that it is confined mainly to the ligand system.

Powder EPR spectra gave isotropic g values (2.0036) near the free-electron value, and the X-ray photoelectron spectra support the lack of any Ni(I) character in **6**: the nitrogen and nickel binding energies seem unaffected, within the experimental error, by reduction (Table VII); that is the extra electron in **6** is delocalized over the whole complex molecule and, therefore, only a small fraction over the nickel atom.

Finally, a metal redox process, going from **5** to **6**, may reasonably be excluded on energetic grounds, since Zn(β-dtpy)$_2$ is reduced at essentially the same potential as **5**.[32]

4. Conclusion

The truly new Ni(β-dtpy)$_2$ complex resembles NiPc in electronic structure and TCNQ in redox behavior for the high degree of substitution with cyano groups. It can be easily reduced to radical-monoanion Ni(β-dtpy)$_2^{\bullet-}$ in either a protic or aprotic solvent, and the ligand is the part preferably involved in the reduction. Ni(β-dtpy)$_2^{\bullet-}$ forms two kinds of complexes after combination with different cations: (a) semiconductor, simple salts with cations of low electrophilicity (for example NEt_4^+), and (b) neutral, mixed stack, charge-transfer compounds with reducible cations (for example $TTF^{\bullet+}$). In order to exploit fully the analogy with $TCNQ^{\bullet-}$, we are trying to synthesize mixed-valence complex salts, producing the anion Ni(β-dtpy)$_2^{\bullet-}$ in the presence of special cations that are less easily reducible than $TTF^{\bullet+}$.

Acknowledgment. We thank Dr. D. Attanasio for the EPR spectra, Dr. G. Righini and Mr. G. Cossu for the ESCA measurements, Mr. C. Veroli for drawings and technical assistance, and the Progetto Finalizzato Materiali Speciali del CNR for financial support.

Registry No. **3**, 134028-83-4; **4**, 134028-85-6; **5**, 122068-18-2; **6**, 134028-86-7; **7**, 134028-88-9; Ni(β-dtpy)$_2^{\bullet-}NEt_4^+$, 134028-81-2; Ni$(C_{11}N_7H_2)_2^{\bullet-}$, 134028-80-1.

Supplementary Material Available: For **3** and **4**, Tables SI–SVI, listing complete crystal data and experimental details, geometrical and conformational parameters of the dioxane molecules, atomic coordinates and thermal parameters (derived hydrogen positions included), and anisotropic thermal parameters (11 pages); tables of structure factor amplitudes (26 pages). Ordering information is given on any current masthead page.

(23) Peng, S. M.; Ibers, J. A.; Millar, M.; Holm, R. H. *J. Am. Chem. Soc.* **1976**, *98*, 8037.
(24) Thomas, R.; Fendrick, C. M.; Lin, W. K.; Glogowski, M. W.; Chavan, M. Y.; Alcock, N. W.; Busch, D. H. *Inorg. Chem.* **1988**, *27*, 2534.
(25) Shaik, S. S.; Whangbo, M. W. *Inorg. Chem.* **1986**, *25*, 1201.
(26) Bellitto, C.; Bonamico, M.; Fares, V.; Imperatori, P.; Patrizio, S. *J. Chem. Soc., Dalton Trans.* **1989**, 719.
(27) Cremer, D.; Pople, J. A. *J. Am. Chem. Soc.* **1975**, *97*, 1354.
(28) Luo, X. L.; Schulte, G. K.; Crabtree, R. H. *Inorg. Chem.* **1990**, *29*, 683.
(29) Torrance, J. B. *Acc. Chem. Res.* **1979**, *12*, 79.
(30) Acker, D. S.; Hertler, W. R. *J. Am. Chem. Soc.* **1962**, *84*, 3370.
(31) Wagner, C. D.; Davis, L. E.; Zeller, M. V.; Taylor, J. A.; Raymond, R. M.; Gale, L. M. *Surf. Interface Anal.* **1981**, *3*, 211.
(32) Bonamico, M.; Fares, V.; Flamini, A.; Poli, N. Unpublished work.